Dalton Transactions

Accepted Manuscript

This article can be cited before page numbers have been issued, to do this please use: L. Marchiò, N. Marchetti, C. Atzeri, V. Borghesani, M. Remelli and M. Tegoni, *Dalton Trans.*, 2014, DOI:

ROYAL SOCIETY OF CHEMISTRY

www.rsc.org/dalton

Journal Name

RSCPublishing

View Article Online
DOI: 10.1039/C4DT03264K

ARTICLE

The peculiar behavior of Picha in the formation of metallacrown complexes with Cu(II), Ni(II) and Zn(II) in aqueous solution

Cite this: DOI: 10.1039/x0xx00000x

Received 00th January 2012,
Accepted 00th January 2012

DOI: 10.1039/x0xx00000x

www.rsc.org/

Luciano Marchiò,[a] Nicola Marchetti,[b] Corrado Atzeri,[a] Valentina Borghesani,[a] Maurizio Remelli[b] and Matteo Tegoni*[a]

The thermodynamic stability of the metallacrown complexes formed by picolinehydroxamic acid (Picha) with Cu(II), Ni(II) and Zn(II) in aqueous solution has been determined by potentiometry, and the speciation models validated by ESI-MS and UV-visible spectrophotometry. Cu(II) and Zn(II) form 12-MC-4 species as the unique metallacrowns present in solution. While for Cu(II) the 12-MC-4 is slightly less stable than that obtained with alaninehydroxamic acid (Alaha), the opposite was found for Zn(II). Moreover, with Cu(II) unprecedented 15-MC-5 and 18-MC-6 species were identified under ESI-MS conditions. Picha with Ni(II) forms, on the contrary, a 15-MC-5 complex as the unique metallacrown species. Structural studies of the framework of the 12-MC-4 complexes by *ab initio* methods were also carried out. The results of our investigations allowed to rationalize not only the different behaviour of Picha in the formation of metallacrowns with the three metal ions, but also the reasons which underpin the strategies of stabilization of these species reported in the literature using ancillary ligands such as pyridine.

Introduction

The use of transition metal-ligand systems is known as a proficient approach for the design of supramolecules with desired geometries and properties.[1–5] Metallacrowns (MCs) are among the earliest identified supramolecules based on transition metals-ligands building blocks.[6–9] MCs are the inorganic analogs of the organic crown ethers, and contain an oxygen-rich cavity into which metal ions such as transition metals, alkali, earth-alkali metals, lanthanides and heavy metals can be encapsulated (Scheme 1).[10–12] To obtain these assemblies perhaps the most widely used ligands are aminohydroxamates, which contain both an amino and an hydroxamic function.[10–12] Transition metal ions such as copper(II), manganese(II), nickel(II) and zinc(II) were the most employed ring metals in the assembly of metallacrowns (M in Scheme 1), although a number of MCs have been isolated using metals which span over the entire transition metal block, and beyond.[10]

Metallacrowns consist of discrete supramolecular aggregates in which a significant number of metal ions are confined. These metals often possess a series of axial coordination sites available for interactions with solvent molecules or co-ligands.[10–12] For these reasons MCs have been studied as recognition agents for anions and cations,[13–20] as single molecule magnets,[21–23] as building blocks for mesoporous solids,[24] and as luminescent materials for the purpose of *in vivo* imaging.[25,26] Despite the number of structural and functional studies, numerous aspects which regulate the stability of MCs in solution and the correlation between the species isolated in the solid state and those present in the solution phase are far from being fully elucidated.

Perhaps the most important principle for the design of MC scaffolds is the *metallacrown structural paradigm*,[12,27] related to planar metallacrown complexes containing copper(II) or nickel(II), which prefer square planar to elongated octahedral coordination environments. Following this paradigm α-aminohydroxamic acids, in which the amino and hydroxamic functions are separated by one carbon atom, possess a geometry appropriate for the assembly of 15-MC-5 complexes (Scheme 1a). The ligand α-alaninehydroxamate (Alaha, Scheme 2a) belongs to this category. Conversely, β-aminohydroxamates possess the appropriate geometry for the assembly of 12-MC-4, by virtue of the longer spacer between the amino and hydroxamic functions necessary to close a cyclic structure with four ring fragments (Scheme 1b). Our research group presented in the past years a study on the thermodynamics of formation of both 12-MC-4 and 15-MC-5 complexes of copper(II) and nickel(II) with hydroxamic derivatives of α-, β- and γ-derivatives of amino acids.[28–35] Perhaps the most important observation was that in the absence of cations such as calcium(II) or lanthanide(III) ions the α-aminohydroxamates form 12-MC-4 complexes with copper(II), but not 15-MC-5 complexes, which represents an exception to the *metallacrown structural paradigm*.[12,34] By addition of larger Ln(III) or UO_2(VI) ions (M' in Scheme 1) the 12-MC-4 of α-derivatives rearrange into 15-MC-5 complexes.[36–38] In these species, the latter M' ions occupy the central cavity and stabilize the expanded 15-MC-5 scaffold.[30]

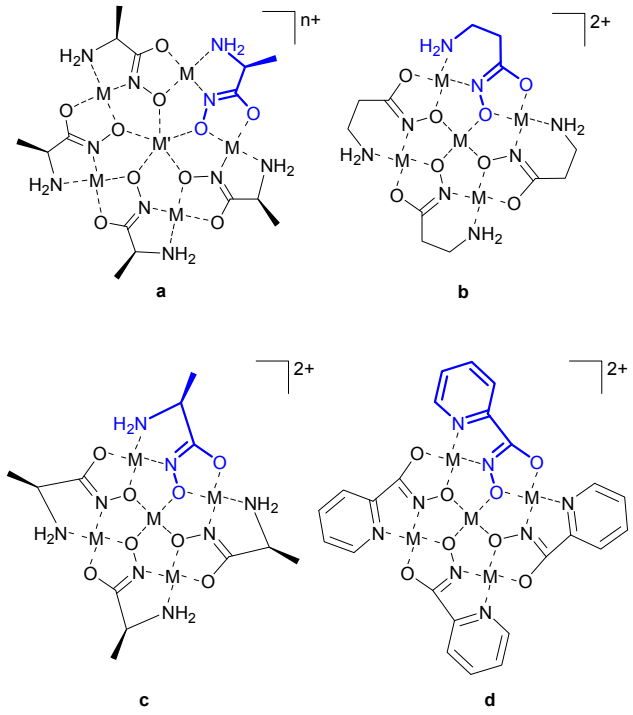

Scheme 1. Representation of metallacrown complexes. (a) 15-MC-5 of α-alaninehydroxamic acid (Alaha). (b) 12-MC-4 of β-alaninehydroxamic acid. (c) 12-MC-4 of Alaha. (d) 12-MC-4 of picolinehydroxamic acid (Picha). M= Cu(II), Ni(II), Zn(II). M'(n) = Ca(II), Ln(III), UO_2(VI).

On the other hand we also observed that, with nickel(II), α-amino acid hydroxamates form both 12-MC-4 and 15-MC-5 complexes even in the absence of suitable core cations.[29] The formation of the latter species was unprecedented for these ligands, and we demonstrated that nickel(II) 15-MC-5 complexes may exist both as cavity-vacant species or as adducts with K(I) or Na(I), likely interacting with the oxygen-rich cavity.[29]

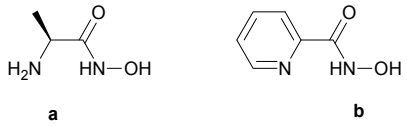

Scheme 2. Schematic representation of the ligands used in this study. (a) α-Alaninehydroxamic acid (Alaha, HL). (b) Picolinehydroxamic acid (Picha, HL).

The structure of the 12-MC-4 complexes of α-aminohydroxamates and their analogues remained elusive for a long time until the zinc(II) and nickel(II) 12-MC-4 of picolinehydroxamic acid (Picha, Scheme 2b) were isolated in the solid state (Scheme 1d).[39] Intriguingly, in these structures several pyridine molecules act as co-ligands occupying one (Zn(II)) or both (Ni(II)) axial coordination positions on the ring metals.[39] On the contrary, attempts to isolate the copper(II) 12-MC-4 complex with Picha in the solid state were unsuccessful, although this MC has been recently identified as the predominant species in methanol:water 8:2 solution.[40] The integrity of the 12-MC-4 complexes of Picha with Zn(II) and Ni(II) has been studied in different solvents,[39] but the thermodynamic aspects which underlie their formation were not yet elucidated. The interest in the equilibria involving Zn(II) metallacrowns resides in the capacity of this metal to form a great variety of metallacrown motifs with Picha as a function of the solvent used and the presence of co-ligands such as pyridine.[26,41,42] This structural promiscuity originates from the preference of Zn(II) for a square-pyramidal geometry which is incompatible with symmetry of planar 12-MC-4 or 15-MC-5 complexes. In this context, the investigation of the binary Zn(II)/Picha system is required to elucidate in the future the the stability of the different assemblies obtained with Zn(II).[42]

In this paper we present our study on the thermodynamics of formation of Cu(II), Ni(II) and Zn(II) metallacrown complexes with picolinehydroxamate in aqueous solution, in particular focusing on the identification of the MC species formed in solution. We also reinvestigated the speciation of the Zn(II)/α-alaninehydroxamic acid (Alaha) system, previously presented in the literature, in light of the possible formation of 12-MC-4 species not reported.[43,44] The comparison of the thermodynamic stabilities of Cu(II), Ni(II) and Zn(II) MC species with Picha and Alaha offers a unique opportunity for a deeper understanding of the relationship between the geometry and the structure of the ligands (more rigid and planar Picha, more flexible Alaha), the geometric preferences of the metals (square-planar or elongated tetragonal for Cu(II) and Ni(II), square pyramidal or octahedral for Zn(II)), and the stability of the MC species formed in solution.

Results

The synthesis of the ligand Alaha was performed from (*S*)-α-alanine through a protection-activation strategy, as depicted in Scheme S1. The protection of the amino group with a carboxybenzyl group was followed by the activation of the carboxylic group and condensation with benzyl-protected hydroxylamine. Catalytic hydrogenation allowed removal of both protecting groups and afforded the pure compound in a moderate yield (see Experimental section).

Table 1. Logarithms of protonation and complex-formation constants of the Cu(II), Ni(II) and Zn(II) complexes with Picha and Alaha. T = 298.2 K, I = 0.1 mol L^{-1} (KCl)

Species	Picha (HL)	Alaha (HL)
HL	8.28(1)	9.15[a]
H_2L	9.92(1)	16.48[a]
$[CuL]^+$	8.69(15)	10.76(1)[a]
$[CuL_2]$	17.67(7)	19.84(1)[a]
$[CuL(LH_{-1})]^-$	9.17(7)	9.82(1)[a]
$[Cu_5(LH_{-1})_4]^{2+}$	38.65(13)	40.16(1)[a]
σ; n	2.47; 270	
$[NiL]^+$	7.15(1)	6.88(1)[b]
$[NiL_2]$	13.78(1)	14.05(1)[b]
$[NiL_3]$-	19.36(2)	-
$[NiL(LH_{-1})]^-$	4.28(4)	4.87(3)[b]
$[Ni_5(LH_{-1})_4]^{2+}$	-	15.51[b]
$[Ni_5(LH_{-1})_5]$	14.92(11)	13.53(8)[b]
σ; n	1.59; 207	
$[ZnLH]^{2+}$	-	12.40(4)
$[ZnL]^+$	5.29(2)	5.30(5)
$[ZnL_2]$	10.41(5)	10.37(3)

$[ZnL_3]^-$	13.75(3)	-
$[ZnL(LH_{-1})]^-$	1.93(3)	1.11(3)
$[Zn_5(LH_{-1})_4]^{2+}$	9.63(5)	6.79(10)
σ; n	2.20; 280	6.42; 550

[a] See ref. [34]. [b] See ref. [29].

The protonation constants of Picha were determined in aqueous solution and are reported in Table 1 along with those of Alaha.[34] The two pK_a values of Picha (1.64 and 8.28) are similar to those reported for the same ligand in methanol/water 80:20.[40] The second pK_a value (8.28) can be ascribed to the dissociation of the NH proton of the hydroxamic group, and it is consistent with the values previously observed for aminohydroxamates.[12,31,45] The first process instead relates with the dissociation of the protonated pyridyl group, and the corresponding pK_{a1} value is remarkably lower than that of alkyl-substituted pyridines (*ca.* 6 for picoline and 2-ethylpyridine)[46], although similar to that determined for picolinamide in aqueous solution (1.9).[47]

The logarithms of the copper(II), nickel(II) and zinc(II) complex formation constants with Picha and Alaha are also reported in Table 1. The data for the Cu(II) and Ni(II) / Alaha systems are those recently published by our group (representative speciation diagrams are reported in Figures S1-3, Supplementary Information).[12,29,31,34] In the literature the speciation of the Zn(II) / Alaha system has already been reported, but the possible formation of metallacrown species was not considered.[43–45] We therefore decided to reinvestigate this system in light of the possible formation of MC complexes.

A marked drift to higher pH was observed during the collection of the potentiometric data of both the Cu(II) and Ni(II) / Picha systems, in the pH ranges 3.0-8.0 for Cu(II) and 6.5-10.5 for Ni(II). In these intervals the systems required up to 45 minutes to reach the equilibrium for each titration point, and the attainment of the equilibrium was assessed by no changes in the e.m.f. reading over 2 minutes. However, no precipitation occurred during the titrations of either the Cu(II) and Ni(II) systems in the entire pH range examined. Interestingly, when the pH of the Cu(II) solutions was raised rapidly from acidic to *ca.* 7, a brown gelatinous precipitate appeared, which then dissolved in few hours upon standing of the solution. This suggested the formation of an insoluble complex, possibly polymeric, which redissolved when the system was left to reach the equilibrium conditions. For the Zn(II) system, the collection of the potentiometric data for ligand:metal ratio lower than 2 was limited to pH 6.2 as at higher values a marked drift of the e.m.f. readings toward lower pH was observed, followed by precipitation of zinc hydroxide when the solution was left stand overnight.

A distribution diagram for the Cu(II) / Picha (HL) system is reported in Figure 1. The speciation model is similar to that in methanol/water 80:20,[40] although the species distribution is very different as a consequence of the different log β in the two solvents (the distribution diagram reported in ref. 40 is drawn for a Cu:L ratio of 1:3 but it does not change for a 1:2.2 ratio). The speciation model is also similar to that of the Cu(II) / Alaha (HL) system in aqueous solution.[12,31,34] The complexation starts well below pH 2 with the $[CuL]^+$ species, followed by the formation of $[CuL_2]$. The formation of the 12-MC-4 complex $[Cu_5(LH_{-1})_4]^{2+}$ starts at pH 2 and the species reaches its maximum amount of *ca.* 37 % total copper at pH 2.9. The formation of significant amounts of 12-MC-4 (> 10%) is limited to the pH range 2-5 by the formation of the $[CuL_2]$ species, which is predominant in the pH range 2-8. At pH higher than 7, the $[CuL_2]$ species deprotonates with the formation of the $[CuL(LH_{-1})]^-$ complex; the pK_a of this process, calculated from the difference between the log β values of $[CuL_2]$ and $[CuL(LH_{-1})]^-$ species, is 8.50(10).

View Article Online
DOI: 10.1039/C4DT03264K

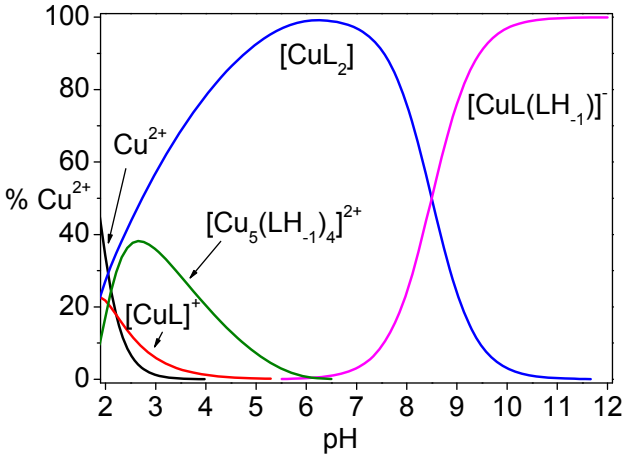

Figure 1. Representative distribution diagram of the system Cu(II) / Picha (HL). Cu:L = 1:2.2, $C_{Cu} = 2.8\times10^{-3}$ mol L^{-1}, I = 0.1 mol L^{-1} (KCl), T = 298.2 K.

In order to characterize the complex species, a series of visible spectra of batch solutions containing Cu(II) and Picha were registered at different pH (Cu:L = 1:2, see Figure S4, Supplementary Information). The spectra in the pH range 2.1-2.8 are dominated by the onset and increase of a band at *ca.* 570 nm attributed to the formation of the 12-MC-4 species (20 to 38% of total copper). At lower pH, the free Cu(II) ion and the $[CuL]^+$ complex predominate, contributing to the band at 680 nm. At pH higher than 7, the only two species present in solution are $[CuL_2]$ and $[CuL(LH_{-1})]^-$. The latter two species absorb at *ca.* 500-520 nm (shoulder), and their interconversion is supported by the presence of an isosbestic point at *ca.* 580 nm. The calculated visible spectra of the four complex species are shown in Figure 2. The maximum of absorbance of the 12-MC-4 species $[Cu_5(LH_{-1})_4]^{2+}$ (581 nm) is consistent with that measured for the same species in methanol:water 80:20 (575 nm),[40] and different from that observed for Alaha (648 nm).[34].The λ_{max} value for the 12-MC-4 with Picha was previously reported in DMSO, and resulted 705 nm.[38] Although without a direct evidence, a partial dissociation of the 12-MC-4 species in DMSO could have occurred, with the formation of $[CuL]^+$ (λ_{max} = 684 nm) which contributes to the absorption at higher wavelengths. The maxima for the species $[CuL_2]$ and $[CuL(LH_{-1})]^-$ are not clearly determined as they fall close or under the tail of a strong absorption at $\lambda < 500$ nm.

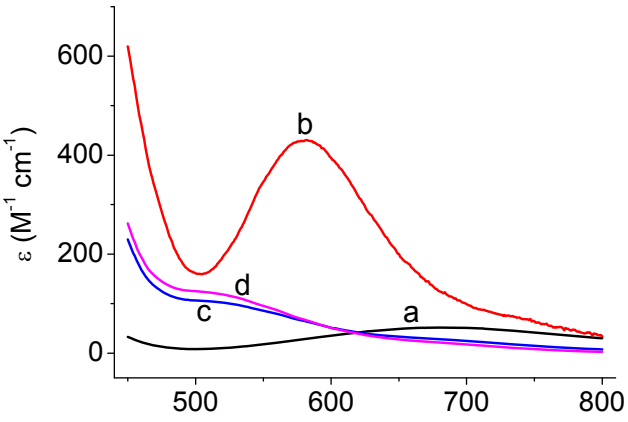

Figure 2. Calculated molar visible spectra for the complex species in the Cu(II) / Picha (HL) system. I = 0.1 mol L^{-1} (KCl), T = 298.2 K. (a) $[CuL]^+$; (b) $[Cu_5(LH_{-1})_4]^{2+}$; (c) $[CuL_2]$; (d) $[CuL(LH_{-1})]^-$.

In an attempt to confirm the presence of the 12-MC-4 complex, ESI-MS spectra at pH 2.3, 6.0 and 11.3 were collected in positive ion mode using a Cu(II):Picha ratio of 5:6 mM. At pH 2.3 the 12-MC-4 complex was detected as $[Cu_5(LH_{-1})_4]^{2+}$ (*m/z* = 430) and as its adduct with the chloride ion ($[Cu_5(LH_{-1})_4]Cl^+$, *m/z* = 896), while the only mononuclear complex identified was $[CuL_2]$ (as $[CuL_2]H^+$ at *m/z* = 338), (Figures S11 and S12, Supplementary Information). Quite surprisingly, when the pH was increased (first to 6.0 and then to 11.3) the most abundant ions were those of the species $[Cu_5(LH_{-1})_5]Na^+$ (*m/z* 1019), $[Cu_5(LH_{-1})_5]K^+$ (*m/z* 1035) and $[Cu_6(LH_{-1})_6]K^+$ (*m/z* 1236), as confirmed by their isotopic pattern (Figures S12 and S13 Supplementary Information). The stoichiometry of these species correspond to those of 15-MC-5 and 18-MC-6 as their adducts with either Na^+ or K^+ ion, respectively.

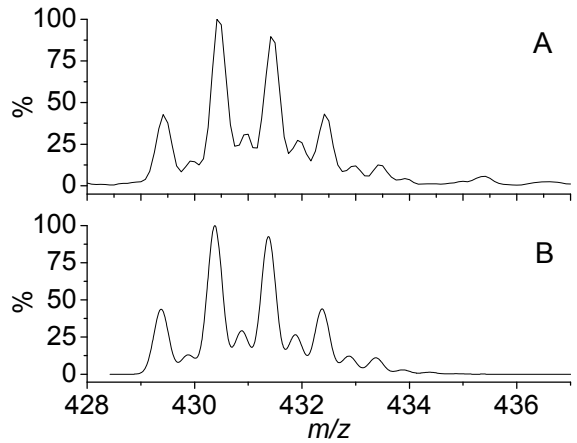

Figure 3. Experimental (a) and simulated (b) ESI–MS spectrum for the complex $[Cu_5(LH_{-1})_4]^{2+}$, in the system Cu(II) / Picha (HL). Cu:L = 5:6, C_{Cu} = 5×10^{-3} mol L^{-1}, pH 2.3.

The 15-MC-5 and 18-MC-6 species were not previously identified in the ESI-MS spectra of the Cu(II) / Alaha system.[34] We therefore decided to treat the potentiometric data of the Cu(II) / Picha system by introducing these species in the model, either alone, or in combination with the 12-MC-4 species. Refinement of the formation constants was only obtained when the 12-MC-4 species $[Cu_5(LH_{-1})_4]^{2+}$ was introduced in the speciation model as the sole metallacrown species, therefore leading us to propose the model reported in Table 1.

The speciation model of the Ni(II) / Picha system is reported in Table 1, and the corresponding distribution diagram is drawn in Fig. 4. The speciation of the Ni(II) / Alaha, previously reported in the literature,[29] is also shown in Table 1. Contrarily from what observed for Cu(II), the models for the two ligands are different. The species $[NiL_3]$ is present only in the Ni(II) / Picha system while, more importantly, the 12-MC-4 species $[Ni_5(LH_{-1})_4]^{2+}$ is absent in this system. The speciation model of the Ni(II) / Picha consists of the $[NiL]^+$ complex which starts to form at pH 2, followed by $[NiL_2]$ at pH 3. These two species reach their maximum, respectively, of *ca*. 46 % total nickel (at pH 3.9) and 63 % (at pH 5.4). The $[NiL_3]^-$ species starts its formation at pH *ca*. 4, but it reaches a maximum of 55 % only at pH 9.4. Finally, the most deprotonated $[NiL(LH_{-1})]^-$ species forms at pH above 7 together with the 15-MC-5 species $[Ni_5(LH_{-1})_5]$ (the latter amounting to *ca*. 38 % total nickel at pH 9.7). The pK_a for the deprotonation of the $[NiL_2]$ species to give $[NiL(LH_{-1})]^-$ resulted 9.50(4).

Previous investigations demonstrated that, for the Ni(II) / Alaha system, two metallacrowns are formed: $[Ni_5(LH_{-1})_4]^{2+}$ and $[Ni_5(LH_{-1})_5]$ corresponding to a 12-MC-4 and 15 MC-5 complexes, respectively.[29] On the contrary, for the Ni(II) / Picha system the 12-MC-4 species does not form, as confirmed by ESI-MS spectra and UV-Vis spectrophotometric data described hereafter. Actually, a satisfactory fitting of the potentiometric curves was obtained both by the introduction in the speciation model of the 15-MC-5 species $[Ni_5(LH_{-1})_5]$ alone, and together with the 12-MC-4 species $[Ni_5(LH_{-1})_4]^{2+}$, obtaining a total sample standard deviation (σ) of 1.59 and 1.31 for the two cases, respectively. However, the improvement of fitting by inclusion of the 12-MC-4 species in the model is limited to 5-6 points only in the curve with Ni(II):Picha = 1:1.46. Importantly, the exclusion from the speciation model of the 15-MC-5 species led to a lack of fitting of the potentiometric curves, thus confirming its formation.

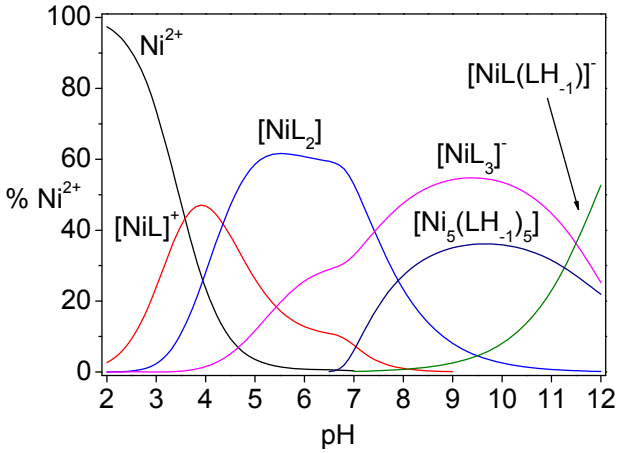

Figure 4. Representative distribution diagram for the system Ni(II) / Picha (HL). Ni:L = 1:2.2, C_{Ni} = 2.4×10^{-3} mol L^{-1}, I = 0.1 mol L^{-1} (KCl), T = 298.2 K.

In an attempt to possibly detect the formation of the 12-MC-4 species we have collected the ESI-MS spectra of a solution containing Ni(II) and Picha in ratio 5:6, at pH 6.9 and 10.3 (Figures S13 and S14, Supplementary Information). The spectra are dominated by the presence of the signals of the

$[Ni_5(LH_{-1})_5]Na^+$ and $[Ni_5(LH_{-1})_5]K^+$ ions (Fig. 5). Both these signals were attributed to the 15-MC-5 species in the form of adducts with the two alkali metals. The signals present in the spectrum remain the same when the pH is increased to 10.3. Perhaps most importantly, no signals associated to the species $[Ni_5(LH_{-1})_4]^{2+}$ (*m/z* = 417) or $[Ni_5(LH_{-1})_4]Cl^+$ (*m/z* = 872) were observed in the spectra at either of the pH conditions. The absence of the 12-MC-4 species was unexpected also because the structure of the $[Ni_5(LH_{-1})_4]^{2+}$ complex with quinolinehydroxamic acid (Quinha), very similar to Picha, was reported recently for crystals obtained from a DMF/pyridine solution.[39] The complex has pyridine molecules coordinated to the axial positions of Ni(II) on both MC faces, and its integrity has been demonstrated in various solvents which however did not include water.

A series of visible spectra on solutions containing Ni(II) and Picha in ratios 2.73 and 1.45, at different pH were collected. The spectra are reported in Figures S5 and S6 (Supplementary Information), while the calculated molar spectra of the complexes are reported in Figure 6. The spectroscopic data were treated taking into account both the model reported in Table 1 and the model which includes the 12-MC-4 complex $[Ni_5(LH_{-1})_4]^{2+}$ (Supplementary information, Table S1). The molar absorbances of all complexes formed by Ni(II) with Picha resulted significantly lower (*ca*. 80 %) than those of the corresponding species with Alaha.[29] Using the model of Table S1 we calculated the molar spectra of the Ni(II) complexes (Figure S7, Supplementary Information) which however were not significantly different to those in Figure 6. The molar spectrum of the putative 12-MC-4 species should have a band centered at 612 nm (ε= 46 M^{-1} cm^{-1}, Fig. S7), while the absorption maximum of the 15-MC-5 is *ca*. 558 nm on a shoulder (ε= 66 M^{-1} cm^{-1}).

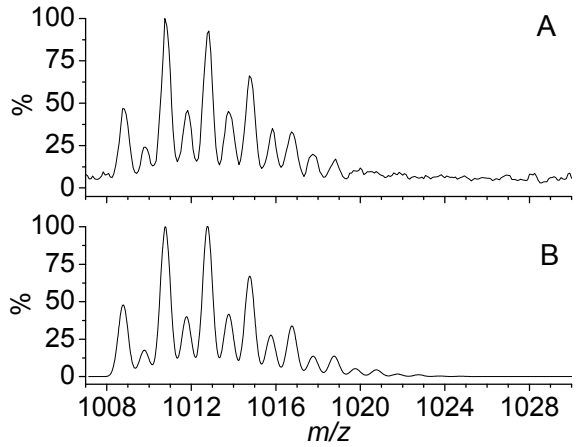

Figure 5. Experimental (a) and simulated (b) ESI–MS spectrum for the complex $[Ni_5(LH_{-1})_5]K^+$ (*m/z* = 1013), in the system Ni(II) / Picha (HL), at pH 10.3. Ni:L = 5:6, $C_{Ni} = 5\times10^{-3}$ mol L^{-1}.

The careful analysis of these spectra showed that the experimental spectra are not consistent with the presence of the 12-MC-4 species (Figure S6, Supplementary Information), and that its spectrum likely is a calculation artefact. The intensity of the band at *ca*. 575 nm increases in the pH range 6.14-6.47, followed by a blue shift at pH 7.0. The putative $[Ni_5(LH_{-1})_4]^{2+}$ (λ_{max} = 612 nm), if present, should actually increase in this interval up to 42 % total nickel (calculated using the speciation in Table S1). Therefore the experimental changes in the visible spectra are better explained by an increase in the concentration of the $[Ni_5(LH_{-1})_5]$ species, which is highly absorbing at 575 nm. On the basis of these observations we propose the model reported in Table 1 as that of the Ni(II)/Picha system.

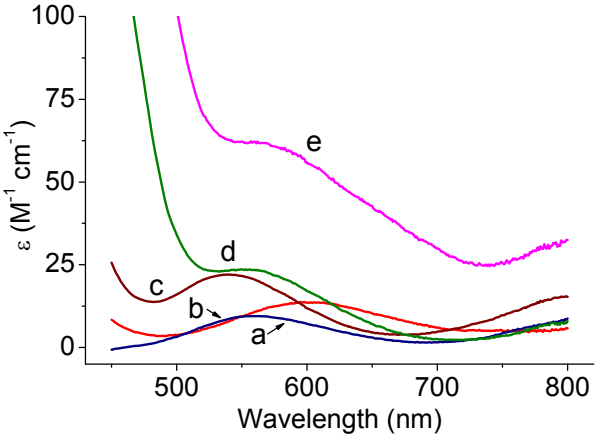

Figure 6. Calculated molar visible spectra for the complex species in the Ni(II) / Picha (HL) system. I = 0.1 mol L^{-1} (KCl), T = 298.2 K. (a) $[NiL]^+$. (b) $[NiL_2]$. (c) $[NiL_3]^-$. (d) $[NiL(LH_{-1})]^-$. (e) $[Ni_5(LH_{-1})_5]$.

The speciation model of the Zn(II) / Picha system (Table 1 and Fig. 7a) consists of four mononuclear complexes ($[ZnL]^+$, $[ZnL_2]$, $[ZnL_3]^-$, $[ZnL(LH_{-1})]^-$) and the 12-MC-4 species $[Zn_5(LH_{-1})_4]^{2+}$. In order to compare this speciation model with that of Zn(II)/Alaha, we decided to carry out the reinvestigation of the latter system in the attempt to possibly identify the presence of MC species previously not reported.[43,44] Actually, we found the formation of a 12-MC-4 complex $[Zn_5(LH_{-1})_4]^{2+}$, together with the four mononuclear species $[ZnLH]^{2+}$, $[ZnL]^+$, $[ZnL_2]$, and $[ZnL(LH_{-1})]^-$ (Table 1 and Fig. 7b).

The speciation models for the systems containing Zn(II) and Picha or Alaha differ for the two mononuclear $[ZnLH]^{2+}$ (with Alaha) or $[ZnL_3]^-$ (with Picha) species, but not for the metallacrown complex $[Zn_5(LH_{-1})_4]_{2+}$ (Table 1). In the Zn(II)/Picha system the complexation starts at pH 3.5 with formation of the $[ZnL]^+$ complex (formation maximum: 37 % at pH 5.3), followed by the $[ZnL_2]$ complex, which reaches a maximum of 58 % total zinc at pH *ca*. 7. At pH higher than 5.5 the formation of the $[ZnL_3]^-$ complex occurs, which reaches 30 % of total zinc at pH 8.5. The $[ZnL(LH_{-1})]^-$ complex starts to form only above pH 6.5. As it regards the 12-MC-4 complex $[Zn_5(LH_{-1})_4]^{2+}$, its formation for a Picha:Zn(II) ratio of 2.2 (Figure 7a) starts at pH 5, and it reaches a maximum at pH 6.4 (28 % of total zinc). A higher formation extent of the 12-MC-4 species can be obtained for a Picha:Zn(II) ratio of 1.5 (38 % at pH 6, data not shown), although the system cannot be investigated at higher pH due to the marked e.m.f. drift and hydroxide precipitation.

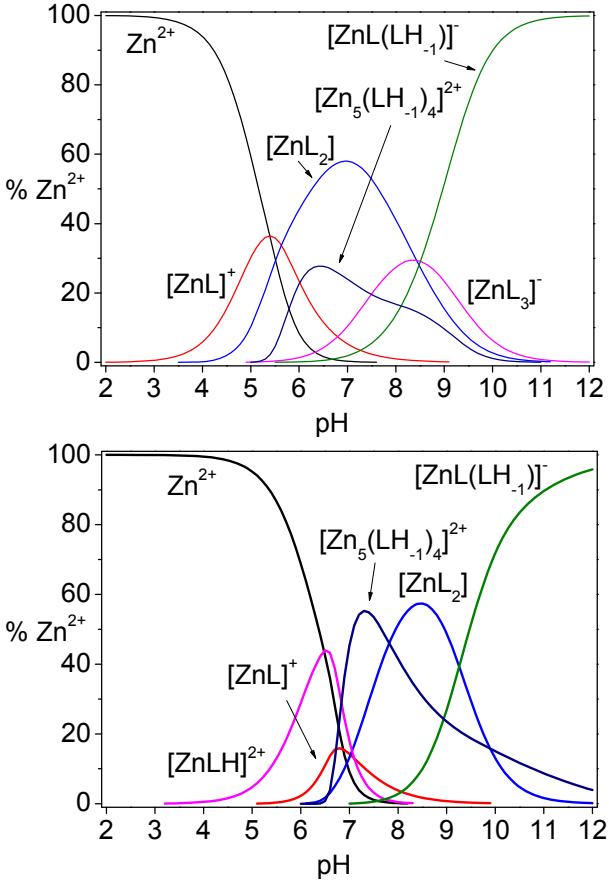

Figure 7. Representative distribution diagrams for the systems Zn(II) / Picha (HL) (above) and Zn(II) / Alaha (HL) (below). Zn:L = 1:2.2, C_{Zn} = 2.8 10^{-3} mol L^{-1}, I = 0.1 mol L^{-1} (KCl), T = 298.2 K.

The presence of the 12-MC-4 complex in the speciation of the Zn(II) / Picha system has been confirmed by ESI-MS data (Figure 8 and Figures S15-S20, Supplementary Information). The signal of the $[Zn_5(LH_{-1})_4]^{2+}$ ion (m/z = 435) is the base peak in the spectrum of Fig. S19, where the Zn(II):Picha ratio is 8:8; its identity is confirmed by the corresponding isotopic pattern (Fig. 8). The ions $[ZnL_2]H^+$ (m/z = 339), $[ZnL_2]Na^+$ (m/z = 361) and $[ZnL_3]^-$ (m/z = 474) were also detected for Zn(II):Picha (the latter ion in negative-ion mode). In 1:1 conditions we also observed an intense signal at m/z = 575, which possess an isotopic pattern consistent with that expected for a $[Zn_6(LH_{-1})_5](OH)_2Na_2^{2+}$. We can tentatively assign this stoichiometry to a 15-MC-5 complex ($[Zn_5(LH_{-1})_5]$), which encapsulates either the sixth Zn(II) ion or one Na^+. By analogy with what observed for the signals observed for the 15-MC-5 complex of Ni(II)/Picha, we suggest that Na^+ can be the ion interacting with the cavity. A second Na^+ and a partially hydrolyzed Zn(II) ion (as $[Zn(OH)_2]$) may interact with the peripheral oxygen atoms of the MC scaffold.

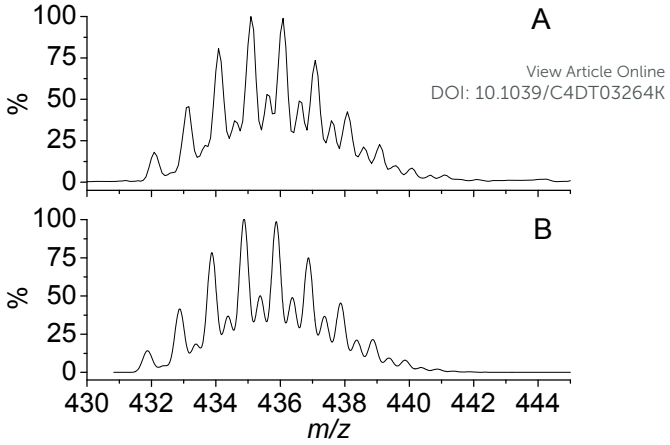

Figure 8. Experimental (a) and simulated (b) ESI–MS spectrum for the complex $[Zn_5(LH_{-1})_4]^{2+}$ (m/z = 435), in the system Zn(II) / Picha (HL), at pH 6.3. Zn:L = 8:8, C_{Zn} = 5 10^{-3} mol L^{-1}.

The crystal structure of the 12-MC-4 of Zn(II) and Picha has been recently reported.[39] As the analogous complex of Ni(II) with Quinha, the crystals of the zinc MC were obtained from a DMF/pyridine solution, and pyridine molecules act as axial co-ligands on Zn(II). However, unlike what observed for Ni(II), in the case of Zn(II) our ESI-MS data support the formation of the $[Zn_5(LH_{-1})_4]^{2+}$ also in aqueous medium and in the absence of pyridine. We performed a detailed analysis of the potentiometric data and we observed that the exclusion of the 12-MC-4 species from the speciation model does not allow to fit satisfactorily the potentiometric curves (the σ value raised from 2.02 to 9.26). We also treated the potentiometric data including the species $[Zn_4L_2(LH_{-1})_2]^{2+}$ (which corresponds to the collapsed metallacrown isolated with Picha in the presence of acetate ions[39]) and with the $[Zn_6(LH_{-1})_5]^{2+}$ complex observed in the ESI-MS spectra. The inclusion of the former $[Zn_4L_2(LH_{-1})_2]^{2+}$ species in the model (actually not observed in our ESI-MS spectra) as an alternative species to the 12-MC-4 complex led to a satisfactorily fitting of the potentiometric data, although worse than with the inclusion of the 12-MC-4 complex (σ = 2.92). If treated together with the $[Zn_5(LH_{-1})_4]^{2+}$ species the convergence process resulted however in the rejection of the $[Zn_4L_2(LH_{-1})_2]^{2+}$ species. Furthermore, the refinement of the potentiometric data with the $[Zn_6(LH_{-1})_5]^{2+}$ complex species in place of the 12-MC-4 allowed an equally good fitting of the titration curves. The treatment of the data with both polynuclear complexes ($[Zn_5(LH_{-1})_4]^{2+}$ and $[Zn_6(LH_{-1})_5]^{2+}$) resulted in no convergence. Therefore, on the basis of the relative intensity of the species in the ESI spectra, and on the basis of the potentiometric data treatment, we propose for the Zn(II)/Picha system the speciation model reported in Table 1.

As it regards the Zn(II)/Alaha system, the species $[ZnLH]^{2+}$ starts to form at pH 3.8 and reaches a maximum at pH 6.4 (45 % of total zinc) (Fig. 7, below). The species $[ZnL]^+$ and $[ZnL_2]$ reach 16 % and 57 % of total zinc at pH 6.8 and 8.6, respectively, while the formation of $[ZnL(LH_{-1})]^-$ starts at pH 7. In this system, the 12-MC-4 species $[Zn_5(LH_{-1})_4]^{2+}$ starts to form at pH 6.5, reaching a maximum at pH 7.3 (54 % of total zinc). Finally, the pK_a of the $[ZnL_2]$ complex to give $[ZnL(LH_{-1})]^-$ resulted 9.26.

For the Zn(II)/Alaha system, ESI-MS spectra were collected on aqueous solutions with metal/ligand ratio of 5:6, at pH 7.2 (Figure S20, Supplementary Information): the signals attributable to the $[ZnL_2]H^+$ and $[Zn_5(LH_{-1})_4]^{2+}$ ions (m/z = 272

and 367, respectively) were observed. No other signal possesses an isotopic pattern associated to a Zn(II) complex, with the exception of a signal at *m/z* = 1043. This peak can be tentatively assigned to a $([Zn_6L_6H_{-6}]K)_2^{2+}$ complex, which interestingly has the same stoichiometry of a possible dimer of an 18-MC-6 species. The treatment of the potentiometric data with the 18-MC-6 in place of the 12-MC-4 complex resulted however into no convergence of data treatment. We therefore propose the for the Zn(II)/Alaha the model reported in Table 1.

The model complexes $[Cu_5(LH_{-1})_4]^{2+}$, $[Ni_5(LH_{-1})_4]^{2+}$ and $[Zn_5(LH_{-1})_4]^{2+}$ (HL = Picha) were optimized starting from the the X-ray experimental geometry of the $[Zn_5(LH_{-1})_4](OTf)_{1.25}(OH)_{0.75}(Py)_6(OH_2)_{2.5}$ metallacrown.[39] The pyridine residues of the latter complex were removed for the geometry optimization of $[Cu_5(LH_{-1})_4]^{2+}$, $[Ni_5(LH_{-1})_4]^{2+}$, and $[Zn_5(LH_{-1})_4]^{2+}$ in order to investigate the role played by the metal ions and ligand structure in the overall MC assembly. The absence of ancillary ligands in the metal coordination sphere imposed an approximately square planar geometry for the five metals within each MC unit, which is a non-ideal geometry for zinc(II). The hypothesized molecular structures of the $[Cu_5(LH_{-1})_4]^{2+}$, $[Ni_5(LH_{-1})_4]^{2+}$, and $[Zn_5(LH_{-1})_4]^{2+}$ complexes (HL = Picha) are reported in Figure 9. $[Cu_5(LH_{-1})_4]^{2+}$ and $[Ni_5(LH_{-1})_4]^{2+}$ exhibit similar structures characterized by an overall bowl shape with the four pyridine residues pointing to the same side. The central metal lies at the bottom of the bowl with a distance of approximately 0.8 Å from the mean plane generated by the four peripheral metals. Conversely, $[Zn_5(LH_{-1})_4]^{2+}$ presents a puckered structure with opposite pyridine residues pointing on the same side and vicinal pyridine residues pointing to opposite directions (Figure 9). The reason for the two different molecular arrangements is a consequence of the nearly square planar geometry which is accessible for Cu(II) and Ni(II) in $[Cu_5(LH_{-1})_4]^{2+}$ and $[Ni_5(LH_{-1})_4]^{2+}$, whereas, in the absence of ancillary ligands and with a coordination number of four, Zn(II) tends to adopt a tetrahedral geometry, which causes the MC distortion from the bowl shape. In fact, in $[Cu_5(LH_{-1})_4]^{2+}$ and $[Ni_5(LH_{-1})_4]^{2+}$ the central metal is located at the bottom of the molecular bowl whereas in $[Zn_5(LH_{-1})_4]^{2+}$ it is shifted upwards so that the five metals are lying approximately on a plane (maximum deviation from the mean plane is of 0.41 Å). Finally, a comparison can be made between $[Cu_5(LH_{-1})_4]^{2+}$ with Picha and with valinehydroxamic acid (Valha, similar to Alaha) previously published.[31] This comparison is possible according to the fact that both Alaha (or Valha) and Picha exhibit the same sequence and type of donor atoms. The main difference is the different degree of flexibility expected for the two ligands: Picha seems less suited to assemble a 12-MC-4, as it exhibits a quite rigid structure according to the presence of the sp^2 hybridization for all of the atoms composing its structure. On the other hand, Alaha is more flexible and can better adapt to the metal ion steric requirement (Figures 9 and S9, Supplementary information). Finally, the difference between the stereoelectronic properties of the three metal ions is reflected in the different bond distances between the donor atoms and the metals, and it likely intervenes in determining the relative stabilities of the MCs. In fact these are in line with the ionic radii of the metal ions, which vary in the following order, $Ni^{2+} < Cu^{2+} < Zn^{2+}$ (Figure 9).[48]

PLEASE PLACE FIGURE 9 HERE

Figure 9. Depiction of the optimized molecular structures of the 12-MC-4 with Picha (HL) $[Ni_5(LH_{-1})_4]^{2+}$ (a), $[Cu_5(LH_{-1})_4]^{2+}$ (b), and $[Zn_5(LH_{-1})_4]^{2+}$ (c) with relevant bond distances (Å). Top view (above) and side view (below). B3LYP/3-21G.

View Article Online
DOI: 10.1039/C4DT03264K

Discussion

Protonation and binary complex-formation equilibria

The ligand Alaha is more basic than Picha for both the first and the second dissociation processes (Table 1). For Alaha the two pK_a values (representing the proton dissociation macroconstants) are close to each other and the amino group is more acidic than the hydroxamic group, as shown by the related microequilibria presented previously in the literature.[31,49] In Picha the proton dissociation equilibria are on the contrary well separated by each other. The log β values reported in Table 1 show that the hydroxamic group in Picha is *ca*. 7 times (0.87 log units) more acidic than that of Alaha. On the other hand, the pyridyl group of Picha, is *ca*. 6 orders of magnitude less basic than the amino group of Alaha. We ascribe the lowest value of the pK_{a1} of Picha to peculiar electronic effects arising from the linkage between the pyridyl moiety and the hydroxamic group. Furthermore, the formation of an intramolecular hydrogen bond between the hydroxamic OH and the pyridyl nitrogen may also play a role in disfavouring the protonation of the latter (see Scheme S2). The lower basicity of the pyridyl group of Picha compared to that of the NH_2 group in Alaha affects significantly the complex formation behaviour of Picha, as discussed hereafter. Because the pyridyl nitrogen is available for metal coordination at very acidic pH, the formation of the complex species with Picha starts at a low acidic pH for all metals, namely 2-3 pH units lower than their Alaha analogs, athough the complexes are less stable than those of Alaha.[34]

We have previously shown that, in mononuclear complexes, the 5-membered (*N,N*) chelation is preferred for Alaha (Scheme S3).[34] Because the pyridyl group in Picha is less basic than the amino group, we propose a preference for the (*N,N*) chelation over the (*O,O*) hydroximic coordination also for Picha. On this side, it is worth noting that the $[CuL]^+$ species presents a similar λ_{max} of absorption (684 nm for Picha and 700 for Alaha[34]) therefore suggesting a similar coordination mode. The absorption maxima of the $[CuL_2]$ and $[CuL(LH_{-1})]^-$ species of Picha fall at *ca*. 500-515 nm, again fully consistent with those observed for the same species with Alaha (540 and 496 nm for the two species, respectively).[34] Finally, the pK_a of the $[CuL_2]$ species to give $[CuL(LH_{-1})]^-$ is 8.50 for Picha and 10.02 for Alaha where one hydroximic OH results deprotonated and uncoordinated.[12] The lower value is accounted for by the more acidic behavior of Picha compared to Alaha, although the planarity of the former ligand may also contribute to the stabilization of the square planar $[CuL(LH_{-1})]^-$ complex with possible formation of a strong intramolecular hydrogen bond between the two hydroxamic moieties, as observed previously for Alaha and glycinehydroxamate.[29,50]

The speciation of the Ni(II)/Picha system differs from that of Ni(II)/Alaha for the formation of the $[NiL_3]^-$ species and the absence of the 12-MC-4 complex $[Ni_5(LH_{-1})_4]^{2+}$. The formation of the 1:3 species only with Picha is consistent with the greater capacity of Py-containing ligands to give rise to 1:3 complexes with this metal ion. Actually, if we evaluate the logK_3 values for ethylenediamine (en), picolinamine (Pyam) and 2,2'-bipyridine (Bipy, see Scheme S4), they increase from the former ligand to the latter (4.07, 5.2 and 6.3, respectively). In the Ni(II)/Picha system (L:Ni ratio = 2.2) the $[NiL_3]^-$ species

reaches however only 55 % total nickel as a consequence of the simultaneous formation of the 15-MC-5 complex $[Ni_5(LH_{-1})_5]$.

The speciation models of Picha and Alaha with Zn(II) differ for the formation of the two species $[ZnL_3]^-$ (with Picha) and $[ZnLH]^{2+}$ (with Alaha) (Table 1). As it concerns the former complex, the reason for its formation only with Picha can be accounted for the presence of the pyridyl group. As found for Ni(II), also with zinc(II) the complexation log K_3 values for en, Pyam and Bipy increase in this sequence (2.36, 2.90 and 3.67, respectively)[46]. On the other hand, the presence of the $[ZnLH]^{2+}$ species only in the system with Alaha is explained with the presence of a (O,O^-) chelation mode of the ligand, where the amino group remains protonated. This coordination mode is consistent with that proposed previously in the literature for this species.[43] By virtue of the low basicity of the pyridyl group in Picha, the $[ZnLH]^{2+}$ species is not observed with this ligand and the zinc complexation starts with the formation of the $[ZnL]^+$ complex. For Alaha, the pK_a of $[ZnLH]^{2+}$ to form $[ZnL]^+$ is 7.10, only slightly lower than the pK_a of the amino group in the free ligand (7.33). Therefore, the presence of an (O,O^-) coordination in the $[ZnL]^+$ species or the presence of a mixture of (O,O^-) or (N,N^-) coordination modes in both the $[ZnL]^+$ and $[ZnL_2]$ species of Alaha cannot be excluded. Finally, the $[ZnL_3]^-$ species forms only with Picha, and we put forward the hypothesis that the coordination mode in this complex is (N,N^-).

Metallacrown complexes

All three metal ions form polynuclear complexes with Picha; they correspond to 12-MC-4 (copper and zinc) or 15-MC-5 (nickel) species.

The stability of the 12-MC-4 complex $[Cu_5(LH_{-1})_4]^{2+}$ of Picha is 1.5 log units lower than that of Alaha; despite this, the 12-MC-4 complex with Picha starts to form at much lower pH than that of Alaha (pH *ca*. 1.5). This occurs by virtue of the low basicity of the pyridyl group. This behavior is quantitatively described by the log$K$* for the proton displacement equilibrium 5 Cu(II) + 4 H_2L^+ = $[Cu_5(LH_{-1})_4]^{2+}$ + 12 H^+. The values are -1.03 for Picha and -25.76 for Alaha and show that metal-proton competition is significantly in favor of copper(II) for Picha with respect to Alaha (more than 24 orders of magnitude!). However, due to the simultaneous formation of the $[CuL_2]$ species, also favored by the low basicity of the pyridyl group, the amount of 12-MC-4 with Picha does not go above 37 % total copper (Fig. 1), while the formation of the 12-MC-4 species with Alaha reaches 75 % total copper at pH *ca*. 5 (Figure S1).

The log β values for the $[CuL]^{2+}$ complexes of the ligands series en, Pyam and Bipy are 10.49, 9.5 and 8.12, respectively.[46] This series suggests that the copper 12-MC-4 with Picha is intrinsically less stable than that with Alaha by virtue of the different nature of the ligands. The reasons for the lower stability of the former were accounted by the results of ab initio studies. They actually highlighted that the sp^2 nature of the ligand results in a more tensioned framework of the 12-MC-4 with Picha than with Valha or Alaha.[31] The lower log β value for the 12-MC-4 with Picha compared to that of Alaha is therefore the result of two factors: the lower stability provided by the presence of the pyridyl residue, and the intrinsic tension of the MC framework.

The overall complex-formation behaviour of Picha and of Alaha towards Cu(II) can be analyzed through a competition diagram of a ternary solution containing Cu(II):Picha:Alaha = 1:1:1 in the absence of mixed-ligand complexes. In the graph of Figure 10, P stands for Picha and A for Alaha in their L^- forms.

In the pH range 3-5 the predominant species is the 12-MC-4 of Picha (*ca*. 87 % of total copper at pH 4.1). The formation of this species is not limited here by the formation of the $[CuP_2]$ species because the Cu(II):Picha ratio is set to 1. At neutral pH the two predominant species are $[CuP_2]$ and $[CuA_2]$, which deprotonate at higher pH to give the $[CuP(PH_{-1})]^-$ and $[CuA(AH_{-1})]^-$ species. Remarkably, the diagram shows the absence of the $[Cu_5(AH_{-1})_4]^{2+}$ complex (i.*e.* the 12-MC-4 species of Alaha) in favour of the corresponding Picha metallacrown. The low basicity of Picha accounts for the prevalence of the $[Cu_5(PH_{-1})_4]^{2+}$ species at acidic pH. This occurs in a pH range (4-6) where, in the Cu(II)/Alaha binary system, the Alaha-containing 12-MC-4 is the predominant species (Figure S1).

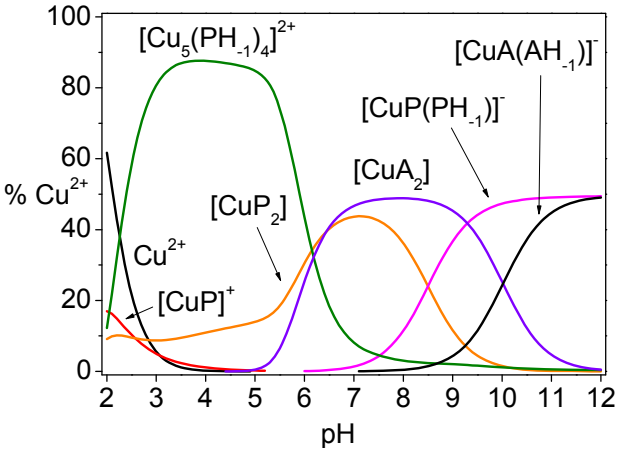

Fig. 10 Representative competition diagram for the system Cu(II) / Picha (HP) / Alaha (HA). Cu:P:A = 1:1:1, C_{Cu} = 2.8 10^{-3} mol L^{-1}. The log β values of the species are reported in Table 1.

Despite the slightly lower log β values of the 12-MC-4 species, Picha exhibits a peculiar tendency to form MC complexes. This is evidenced by two observations, where the first is the small difference between the log β values of the 12-MC-4 complexes of Picha and Alaha (1.5 log β units) irrespective of the geometric strain in the MC with the former ligands, as discussed above. The second observation relates with the presence of ions associated to to 15-MC-5 and 18-MC-6 species in the ESI-MS spectra. Their adducts with Na^+ and K^+ are predominant in the mass spectra: these species are not present in solution at the equilibrium and nevertheless they seem stable under ionization conditions. We have previously demonstrated that the presence of alkali metals (Na^+ and K^+) results in an enhanced stability of the Ni(II) 15-MC-5 species of Alaha,[29] and in the literature it has been reported the isolation of the Na[15-MC-5] complex of Picha and Cu(II).[51] Our results therefore suggest that expanded MC frameworks in which the cavity is occupied by alkali metals may result significantly stabilized under appropriate conditions (*e.g.* ionic strength, solvent etc.). Finally, the log β value of the copper(II) 12-MC-4 with Picha in aqueous solution (38.65) was much lower in methanol:water 80:20 (log β = 56.04),[40] consistently with what was previously found for tryptophan- and phenylalaninehydroxamic acids in mixed methanol:water 9:1, which present log β values for the $[Cu_5(LH_{-1})_4]^{2+}$ species much higher than those observed for α-aminohydroxamates in water.[35]

In the case of Zn(II) the log β value of the 12-MC-4 complex of Picha is 2.8 log units higher than that of Alaha (Table 1). Irrespective of its higher stability, the 12-MC-4 of Picha reaches only 28 % of total zinc, while with of Alaha it reaches 59 % (Fig. 7). This is the result of the presence, for the former ligand, of a high amount of the $[ZnL_2]$ species in the same pH range of formation of the 12-MC-4 complex. The higher stability of the 12-MC-4 of Picha compared to that of Alaha is not accounted for by the presence of the pyridyl group, as the log β values for the $[ZnL]^{2+}$ complexes of en, Pyam and Bipy are 5.69, 5.28 and 5.12, respectively.[46] The structural calculations did not otherwise provided further information on the reasons for the greater stability of the 12-MC-4 species with Picha. The optimised structure in the absence of axial ligands on the peripheral ions presents a saddle-shape rather than a bowl-shape conformation (Figure 9), where Zn(II) is coordinated in a distorted tetrahedral environment. Given the preference of Zn(II) for a square pyramidal or octahedral coordination,[†] it is unlikely that the 12-MC-4 adopts the saddle conformation in solution, and therefore the structural calculations do not provide more insight on the higher stability of the 12-MC-4 species with Picha. It is however remarkable that, despite the preference of Zn(II) for geometries which are almost incompatible with the symmetry of planar MC complexes, the 12-MC-4 species is the only polynuclear species found in aqueous solution.[42]

Ni(II) has a unique behaviour with Picha compared to Cu(II) and Zn(II), as it forms only a 15-MC-5 complex and not the 12-MC-4 species. Structures of Ni(II) 15-MC-5 complexes with Picha are known, although they possess metal ions such Pb(II) encapsulated in the cavity.[52] Here the complex can be either vacant or interacting with K^+ ions. The favourable formation of the 15-MC-5 with Picha compared to Alaha reflects into the higher log β value for the former (1.5 log units higher, Table 1).

The *ab initio* calculations on the putative 12-MC-4 complex formed by Ni(II) with Picha suggest a square planar coordination for Ni(II), although the frameworks is expected tensioned. The smaller ionic radius of Ni(II) compared to Cu(II) (0.63 vs. 0.71 Å in a square planar environment)[48] might also prevent, in the case of Ni(II), an optimal interaction with the donor atoms of the less flexible Picha. Overall these factors result in the destabilization of the 12-MC-4 scaffold. As already underlined, the lack of formation of the 12-MC-4 species seems to contradict the successful isolation in the solid state of the 12-MC-4 with quinolinehydroxamic acid (Quinha), which is similar to Picha.[39] In the crystal structure, however, the peripheral Ni(II) ions are 6-coordinated, where two pyridines occupy the two axial positions. The reason of this behaviour is explained by the observation that the ionic radius of Ni(II) increases from 0.63 Å to 0.83 Å when the coordination changes from square planar to octahedral.[48] Therefore, the presence of axial pyridines allows the stabilization of the 12-MC-4 through mitigation of the structural strains.

The peculiar behaviour of Picha and the stabilities of its 12-MC-4 complexes can be rationalized as follows: Ni(II), which is the smallest ion of the series examined, forms with Picha only a 15-MC-5 species into which the metal can adopt a stable square planar coordination, and which results more stable than in the analogous MC with Alaha. The 12-MC-4 complex with Picha does not form in aqueous medium and 0.1 M KCl because there are no co-ligands of sufficient strength to stabilize a 6-coordination environment around the metal. On the contrary, the 12-MC-4 does form in the same conditions with Alaha by virtue of the greater flexibility of the ligand. In the case of Cu(II), the 12-MC-4 is formed with both ligands, and it is the only MC species observed by potentiometry. Its formation occurs also with Picha by virtue of a slightly larger ionic radius of the metal compared to Ni(II), although the lower flexibility of Picha results into a lower stability of the 12-MC-4 compared to that of Alaha. Picha allows also the formation under ESI conditions of species identified as vacant 15-MC-5 and 18-MC-6 complexes which are unprecedented for Alaha. Finally, Zn(II) forms 12-MC-4 species only, although the one of Picha is significantly more stable than that of Alaha. The largest ionic radius of Zn(II) allows a reduction of the structural tensions in the 12-MC-4, which indeed forms in solution. The species with Picha results also significantly more stable than that of Alaha, showing the higher propensity of Picha to form MC species with Zn(II), which reflects also into the numerous structures of metallacrowns with Zn(II) and Ln(III) ions reported in the literature.[25,26,39,42]

Conclusions

Our results underline the peculiar behavior of the ligand Picha, which is a marked capacity to give rise to metallacrown complexes despite the lower coordination capabilities of the pyridyl group compared to the amino group. The presence of high amounts of MC species in solution is however prevented by the lower basicity of the pyridyl group which on one hand allows the metal complexation at low pH, but it also promotes the formation of stable mononuclear species in place of the MC species. The geometric requirements of the coordination metal sites in the 12-MC-4 framework influence the overall stability of the species: in the case of Ni(II) the molecular geometry of Picha prevents the formation of the 12-MC-4 species, but it allows the assembly of a stable 15-MC-5 complex. In the case of Zn(II), Picha allows to assemble a 12-MC-4 species which is more stable than that of Alaha. Finally, with Cu(II) we have found the presence, although only by ESI-MS, of 15-MC-5 and 18-MC-6 species. We suggest therefore that it should be possible, through a wise choice of the conditions, to stabilize unprecedented expanded MC frameworks assembled using Cu(II) and Picha.

Finally, our data explain the capacity of Picha to give rise to stable MC complexes, but also underline that the role of co-ligands such as pyridine is likely not limited in the simple stabilization of certain coordination geometries of the metal, but may impact the overall stability of the MC scaffold.

Experimental

Reagents

Picolinehydroxamic acid (Picha) has been synthesized and purified as previously reported.[26] Where required, further purification of small portions of Picha was carried out as follows: the solid ligand (0.5 g) was suspended in pure ethyl acetate (30 ml) and left under stirring for 15 min. The filtrate was collected and the precipitate treated with ethyl acetate (5 x). The filtrate aliquots were combined and, following solvent removal *in vacuo,* microcrystals of the pure ligands were obtained (yield *ca.* 85 %).

The ligand Alaha was synthesized as reported below (Scheme S1, Supplementary information). The purity of the ligands was checked by potentiometry and NMR spectroscopy and resulted > 99 %. The sample solutions were prepared by

direct weighting of the solid compounds. Standard solutions of KOH, HCl, $CuCl_2 \cdot 2H_2O$, $NiCl_2 \cdot 6H_2O$ and $ZnCl_2$ solutions were prepared from highly pure commercial products (Carlo Erba chemicals). The KOH solution was standardized using potassium hydrogen phthalate, while the titre of the metal solutions was determined using standard EDTA methods, following the procedures reported elsewhere.[53,54]

Synthesis of (*S*)-*N*-carboxybenzyl-α-alanine (1)

(*S*)-α-Alanine (4.00 g, 44.89 mmol) was dissolved into a solution of sodium hydroxide (3.59 g, 89.78 mmol) in 50 mL of water, and the mixture put in an ice bath. A solution of benzylchloroformate (8.3 mL, 58.14 mmol) in 9 mL of toluene was added to the aqueous mixture under stirring. The mixture was kept under stirring at room temperature overnight. The organic layer was removed, and the aqueous layer washed twice with 20 mL of diethyl ether to remove unreacted benzylchloroformate. The aqueous layer was acidified to pH *ca*. 3 with 1 N aqueous HCl, observing the formation of a precipitate. The product was extracted with ethyl acetate (2 x 20 mL). The combined organic fractions were washed with brine, dried with anhydrous Na_2SO_4, and the solvent removed *in vacuo* to obtain a white powder. Yield 4.76 g (48 %). ^{1}H-NMR (300 MHz, D_6-DMSO) δ 12.53 (br, 1H, COOH), 7.60 (d, 1H, C_αNH), 7.34 (m, 5H, Ph), 5.01 (s, 2H, CH_2Ph), 4.00 (q, 1H, C_αH), 1.25 (d, 3H, CH_3). IR ν/cm^{-1}: 3334, 1699, 1684, 690. Calc. for $C_{11}H_{13}NO_4$ C, 59.19; H, 5.87; N, 6.27; O, 28.67. Found C, 59.3; H, 5.9; N, 6.3; O, 28.6.

Synthesis of (*S*)-*N*-carboxybenzyl-α-alanine-O-benzylhydroxamic acid (2)

Benzylhydroxylamine hydrochloride (3.74 g, 21.34 mmol) was suspended in 30 mL of dichloromethane in a Schlenk flask. After the addition of *N*-methylmorpholine (2.57 mL, 25.50 mmol), the formed precipitate was removed by filtration under inert atmosphere. In a separate flask, **1** was dissolved in 20 mL of dry dichloromethane and the flask was put into an ice bath. *N*-Methylmorpholine (2.3 mL, 21.34 mmol) was added to the solution, followed by ethylchloroformate (2.03 mL, 21.34 mmol). A white precipitate appeared which was not removed. The solution of benzylhydroxylamine was added slowly to the suspension at 0 °C, and kept under stirring for 4 h at room temperature. The organic suspension was washed with an aqueous 1 N solution of HCl (2 x 20 mL), an aqueous satd. $NaHCO_3$ solution (2 x 20 mL) and brine. The organic layer was dried with anhydrous Na_2SO_4, and the solvent removed *in vacuo* to obtain a white powder. Yield 4.45 g (64 %). ^{1}H-NMR (300 MHz, D_6-DMSO) δ 11.21 (s, 1H, CONH), 7.51 (d, 1H, C_αNH), 7.3s (m, 10H, 2xPh), 4.97 (s, 2H, CH_2Ph), 4.74 (s, 2H, CH_2Ph), 3.94 (q, 1H, C_αH), 1.17 (d, 3H, CH_3). IR ν/cm^{-1}: 3294, 3183, 1688, 1657, 698. Calc. for $C_{18}H_{20}N_2O_4$ C, 65.84; H, 6.14; N, 8.53; O, 19.49. Found C, 65.8; H, 6.0; N, 8.6; O, 19.5.

Synthesis of (*S*)-α-alanine (Alaha, 3)

The compound **2** (4.45 g, 13.57 mmol) was added to a suspension of 10% Pd/C (0.30 g) in 50 mL of methanol. Hydrogenation was performed overnight in a Parr apparatus using $p(H_2)$ = 1.5 atm. The catalyst was filtered out and the solvent removed *in vacuo*. The product was collected as a white powder sparingly soluble in methanol, washed with methanol and diethy ether, and dried. Yield 0.57 g (40 %). ^{1}H-NMR (300 MHz, D_6-DMSO) δ 3.14 (q, 1H, C_αH), 1.07 (d, 3H, CH_3). IR ν/cm^{-1}: 3193, 1620. Calc. for $C_3H_8N_2O_2$ C, 34.61; H, 7.75; N, 26.91; O, 30.74. Found C, 34.6; H, 7.9; N, 26.8; O, 30.8.

View Article Online
DOI: 10.1039/C4DT03264K

Potentiometry

The potentiometric titrations were carried out in aqueous solution at T = 298.16 ± 0.1 K and I = 0.1 mol L^{-1} (KCl) under a N_2 stream, using 25 mL samples. The potentiometric apparatus for the automatic data acquisition, already described in ref.[53], consisted of a Thermo pH meter 720A connected to a Hamilton combined glass electrode (P/N 238000). The electrode was calibrated in terms of [H^+] by titrating HCl solutions with KOH (hereafter pH = -log [H^+]). The protonation constants of the ligands were determined by alkalimetric titration of three samples (1.1–1.9·10^{-2} mol L^{-1}). For the metal complexation equilibria with Picha, five titrations were carried out with ligand:metal molar ratios from 2.10 to 3.40 for Cu(II) (C_{Cu} = 2.17-3.16 · 10^{-3} mol L^{-1}), 1.48-3.86 for Ni(II) (C_{Ni} = 2.20-3.67 · 10^{-3} mol L^{-1}), and 1.28-4.92 for Zn(II) (C_{Zn} = 1.41-3.17 · 10^{-3} mol L^{-1}). For the Zn(II) complexation equilibria with Alaha, 5 titrations were carried out with ligand:metal molar ratios from 1.50 to 3.0 (C_{Zn} = 1.20-2.73 · 10^{-3} mol L^{-1}) As it concerns the titrations with Cu(II) and Ni(II), L:M ratios higher than 2 were appropriate for observing the formation of mononuclear complexes and MC species during within the same titration. The pH range explored was approximately 2.4–11.1. A marked drift to higher pH was observed in the pH ranges 3.0-8.0 for the Cu(II)/Picha and 6.5-10.5 for the Ni(II)/Picha systems. In these intervals, the attainment of the equilibrium was assessed by observing no changes in the e.m.f. reading over two minutes (for some points, up to 45 min *per* point were required). Using these equilibration times, no precipitation was observed in the entire pH range examined. For the Zn(II) system, the collection of the potentiometric data for ligand:metal ratio lower than 2 was limited to pH 6.2. At higher values a marked drift of the e.m.f. readings toward lower pH was observed, followed by precipitation of zinc hydroxide when the solution was left stand overnight.

Uv-Vis spectrophotometry

Visible absorption spectra were recorded on a Thermo Evolution 260 Bio spectrophotometer using quartz cells of 1 cm path length and a 0.1 mol L^{-1} KCl solution as a reference. The temperature was kept constant at 298.2 K using a Peltier device. The Cu(II) and Ni(II) complexation equilibria were studied through spectrophotometric batch titration. For the study of Cu(II) complexation equilibria, 10 sample solutions (v_{sample} = 5 ml) were prepared with a ligand:Cu(II) ratio of 2.17 (C_{Cu} = 2.31×10^{-3} mol L^{-1}, I = 0.1 M KCl). For the study of Ni(II) complexation equilibria, 10 sample solutions (v_{sample} = 5 ml) were prepared with a ligand:Ni(II) ratio of 2.73, and additional 5 samples with a ligand:Ni(II) ratio of 1.45 (C_{Ni} = 3.67×10^{-3} mol L^{-1}, I = 0.1 M KCl). The pH of the samples was corrected using a standard KOH solution, obtaining samples with pH in the interval 1.94-10.26 (Cu(II)) and 2.94-11.82 (Ni(II)). The samples were left to equilibrate at 298.2 K for 24 h, and then the spectra were collected.

Electrospray-Ionization Mass-Spectrometry (ESI-MS)

ESI mass spectra were recorded on a linear ion trap LTQ XL Mass Spectrometer (Thermo Scientific, Waltham, MA, USA). Data were processed by using the spectrometer software. The measurements were performed on binary metal/ligand solutions

at appropriate pH values, chosen in order to maximize the formation of a single complex species. The samples were prepared in a similar way as described for potentiometric studies without the addition of background electrolyte. The counter-ion was supplied by the base employed to adjust the pH value (NaOH). Direct infusion analyses were always performed at 10 μL/min. Experimental conditions were as follows: spray voltage 3.0 kV; sheath and auxiliary gas 50 and 5 a.u., respectively; capillary temperature 250 °C; source fragmentation auxiliary voltage 40 V; capillary voltage 36 V and tube lens 80 V for mononuclear complexes; capillary voltage 90 V and tube lens 110 V for polynuclear species.

Calculations

Cu(II), Ni(II) and Zn(II) complexation constants were calculated from the potentiometric data using the HYPERQUAD 2006 program.[55] Least-squares treatment was performed by minimization of the sample standard deviation $\sigma = [\Sigma_i w_i(E_i^o - E_i^c)^2/(n-m)]^{½}$, where E_i^o and E_i^c are the observed and calculated e.m.f. values, respectively, n is the number of observations and m is the number of refined parameters. The statistical weights w_i were put equal to $1/\sigma_i^2$, where σ_i is the expected error on each observed e.m.f. value (0.2 mV). A literature pK_w value of 13.77 was employed.[56] For each system, data from different titrations were treated together. The speciation diagrams were plotted with the Hyss program.[57] The UV-visible spectra collected at different pH values were treated using the Specfit/32 program,[58] using as fixed parameters the complex formation constants obtained from potentiometry.

All the structural calculations were performed with Gaussian 03 software.[59] The model complexes $[Cu_5(LH_{-1})_4]^{2+}$, $[Ni_5(LH_{-1})_4]^{2+}$, and $[Zn_5(LH_{-1})_4]^{2+}$ (HL = Picha) were optimized starting from the the X-ray experimental geometry of the $[Zn_5(LH_{-1})_4](OTf)_{1.25}(OH)_{0.75}(Py)_6(OH_2)_{2.5}$,[39] in the absence of the coordinated pyridine co-ligands. The calculation were performed with the gradient-corrected hybrid density functional B3LYP[60,61] and with the 3-21G basis set.[62]

Acknowledgements

The authors thank the University of Parma (FIL 2012), the University of Ferrara (FAR 2011), and the CIRCMSB (Consorzio Interuniversitario di Ricerca in Chimica dei Metalli nei Sistemi Biologici, Bari, Italy). The authors thank the participants of the FP7 Marie Curie IRSES project "Metallacrowns" (https://sites.google.com/site/metallacrowns) for useful discussions.

Notes and references

[a] Department of Chemistry, University of Parma, Parco Area delle Scienze, 17A, 43124 Parma, Italy. E-mail: matteo.tegoni@unipr.it; Tel: +39 0521 905424.

[b] Department of Chemical and Pharmaceutical Sciences, University of Ferrara, Via Fossato di Mortara 17, 44121 Ferrara, Italy.

† Data from the CCDC structural database report *ca*. 1700 structures for a 4-coordinated Zn(II) in a (N_2,O_2) coordination environment, compared to *ca*. 2300 and 3200 structures for a 5- and 6-coordinated Zn(II), respectively, in a (N_2,O_2,X_{1-2}) coordination.

1 R. Chakrabarty, P. S. Mukherjee, and P. J. Stang, *Chem. Rev.*, 2011, **111**, 6810–6918.
2 P. J. Stang, *J. Am. Chem. Soc.*, 2012, **134**, 11829–30.
3 B. J. Holliday and C. A. Mirkin, *Angew. Chem. Int. Ed. Engl.*, 2001, **40**, 2022–2043.
4 M. Fujita, *Chem. Soc. Rev.*, 1998, **27**, 417–425.
5 D. L. Caulder and K. N. Raymond, *Acc. Chem. Res.*, 1999, **32**, 975–982.
6 V. L. Pecoraro, *Inorg. Chim. Acta*, 1989, **155**, 171–173.
7 M. S. Lah and V. L. Pecoraro, *Comments Inorg. Chem.*, 1990, **11**, 59–84.
8 M. S. Lah and V. L. Pecoraro, *J. Am. Chem. Soc.*, 1989, **111**, 7258–7259.
9 C. M. Zaleski, S. Tricard, E. C. Depperman, W. Wernsdorfer, T. Mallah, M. L. Kirk, and V. L. Pecoraro, *Inorg. Chem.*, 2011, **50**, 11348–11352.
10 Mezei, C. M. Zaleski, and V. L. Pecoraro, *Chem. Rev.*, 2007, **107**, 4933–5003.
11 J. J. Bodwin, A. D. Cutland, R. G. Malkani, and V. L. Pecoraro, *Coord. Chem. Rev.*, 2001, **216-217**, 489–512.
12 M. Tegoni and M. Remelli, *Coord. Chem. Rev.*, 2012, **256**, 289–315.
13 J. T. Grant, J. Jankolovits, and V. L. Pecoraro, *Inorg. Chem.*, 2012, **51**, 8034–8041.
14 J. Jankolovits, C.-S. Lim, G. Mezei, J. W. Kampf, and V. L. Pecoraro, *Inorg. Chem.*, 2012, **51**, 4527–4538.
15 J. Jankolovits, J. W. Kampf, S. Maldonado, and V. L. Pecoraro, *Chem. Eur. J*, 2010, **16**, 6786–6796.
16 C. S. Lim, J. Jankolovits, P. Zhao, J. W. Kampf, and V. L. Pecoraro, *Inorg. Chem.*, 2011, **50**, 4832–4841.
17 C. S. Lim, J. W. Kampf, and V. L. Pecoraro, *Inorg. Chem.*, 2009, **48**, 5224–5233.
18 M. Tegoni, M. Tropiano, and L. Marchiò, *Dalton Trans.*, 2009, 6705–6708.
19 M. Tegoni, M. Furlotti, M. Tropiano, C. S. Lim, and V. L. Pecoraro, *Inorg. Chem.*, 2010, **49**, 5190–5201.
20 C.-S. Lim, M. Tegoni, T. Jakusch, J. W. Kampf, and V. L. Pecoraro, *Inorg. Chem.*, 2012, **51**, 11533–11540.
21 A. Deb, T. T. Boron, M. Itou, Y. Sakurai, T. Mallah, V. L. Pecoraro, and J. E. Penner-Hahn, *J. Am. Chem. Soc.*, 2014, **136**, 4889–4892.
22 T. T. Boron, J. W. Kampf, and V. L. Pecoraro, *Inorg. Chem.*, 2010, **49**, 9104–9106.
23 C. M. Zaleski, J. W. Kampf, T. Mallah, M. L. Kirk, and V. L. Pecoraro, *Inorg. Chem.*, 2007, **46**, 1954–1956.
24 C.-S. Lim, J. Jankolovits, J. W. Kampf, and V. L. Pecoraro, *Chem. Asian J.*, 2010, **5**, 46–49.
25 E. R. Trivedi, S. V Eliseeva, J. Jankolovits, M. M. Olmstead, S. Petoud, and V. L. Pecoraro, *J. Am. Chem. Soc.*, 2014, **136**, 1526–1534.
26 J. Jankolovits, C. M. Andolina, J. W. Kampf, K. N. Raymond, and V. L. Pecoraro, *Angew. Chem. Int. Ed. Engl.*, 2011, **50**, 9660–9664.
27 V. L. Pecoraro, A. J. Stemmler, B. R. Gibney, J. J. Bodwin, H. Wang, J. W. Kampf, and A. Barwinski, *Prog. Inorg. Chem.*, 1997, **45**, 83–177.
28 M. Remelli, D. Bacco, F. Dallavalle, E. Lazzari, N. Marchetti, and M. Tegoni, *Dalton Trans.*, 2013, **42**, 8018–8025.

29 D. Bacco, V. Bertolasi, F. Dallavalle, L. Galliera, N. Marchetti, L. Marchiò, M. Remelli, and M. Tegoni, *Dalton Trans.*, 2011, **40**, 2491–2501.
30 F. Dallavalle, M. Remelli, F. Sansone, D. Bacco, and M. Tegoni, *Inorg. Chem.*, 2010, **49**, 1761–1772.
31 M. Tegoni, M. Remelli, D. Bacco, L. Marchiò, and F. Dallavalle, *Dalton Trans.*, 2008, 2693–2701.
32 M. Tegoni, L. Ferretti, F. Sansone, M. Remelli, V. Bertolasi, and F. Dallavalle, *Chemistry*, 2007, **13**, 1300–1308.
33 M. Tegoni, F. Dallavalle, B. Belosi, and M. Remelli, *Dalt. Trans.*, 2004, 1329–1333.
34 M. Careri, F. Dallavalle, M. Tegoni, and I. Zagnoni, *J. Inorg. Biochem.*, 2003, **93**, 174–180.
35 F. Dallavalle and M. Tegoni, *Polyhedron*, 2001, **20**, 2697–2704.
36 T. N. Parac-Vogt, A. Pacco, C. Goerller-Walrand, and K. Binnemans, *J. Inorg. Biochem.*, 2005, **99**, 497–504.
37 A. Pacco, T. N. Parac-Vogt, E. van Besien, K. Pierloot, C. Görller-Walrand, K. Binnemans, and C. Gorller-Walrand, *Eur. J. Inorg. Chem.*, 2005, **2005**, 3303–3310.
38 S. H. Seda, J. Janczak, and J. Lisowski, *Inorg. Chim. Acta*, 2006, **359**, 1055–1063.
39 J. Jankolovits, J. W. Kampf, and V. L. Pecoraro, *Inorg. Chem.*, 2013, **52**, 5063–5076.
40 E. Gumienna-Kontecka, I. A. Golenya, A. Szebesczyk, M. Haukka, R. Krämer, and I. O. Fritsky, *Inorg. Chem.*, 2013, **52**, 7633–7644.
41 J. Jankolovits, J. W. Kampf, and V. L. Pecoraro, *Polyhedron*, 2013, **52**, 491–499.
42 J. Jankolovits, J. W. Kampf, and V. L. Pecoraro, *Inorg. Chem.*, 2014, **53**, 7534–7546.
43 B. Kurzak, H. Kozlowski, and P. Decock, *J. Inorg. Biochem.*, 1991, **41**, 71–78.
44 E. Farkas, J. Szoke, T. Kiss, H. Kozlowski, and W. Bal, *J. Chem. Soc. Dalton Trans*, 1989, 2247–2251.
45 B. Kurzak, H. Kozlowski, and E. Farkas, *Coord. Chem. Rev.*, 1992, **114**, 169–200.
46 R. M. Smith, A. E. Martell and R. J. Motekaitis, NIST Critically Selected Stability Constants of Metal Complexes Database 46, 7.0, Gaithersburg, MD, USA, 2003.
47 H. L. Conley and R. B. Martin, *J. Phys. Chem.*, 1965, **69**, 2914–2923.
48 R. Shannon, *Acta Cryst. A*, 1976, **32**, 751–767.
49 E. Farkas, T. Kiss, and B. Kurzak, *J. Chem. Soc. Perkin Trans. 2*, 1990, 1255.
50 M. Julien-Pouzol, S. Jaulmes, P. Laruelle, S. Carvalho, and E. D. Paniago, *Acta Cryst. C*, 1985, **C41**, 712–715.
51 S. H. Seda, J. Janczak, and J. Lisowski, *Eur. J. Inorg. Chem.*, 2007, **2007**, 3015–3022.
52 S. H. Seda, J. Janczak, and J. Lisowski, *Inorg. Chem. Commun.*, 2006, **9**, 792–796.
53 F. Dallavalle, G. Folesani, R. Marchelli, and G. Galaverna, *Helv. Chim. Acta*, 1994, **77**, 1623–1630.
54 A. I. Vogel, *Qunatitative Inorganic Analysis Including Elementary Instrumental Analysis*, Longmans, London, UK, Third ed., 1962.
55 P. Gans, A. Sabatini, and A. Vacca, *Talanta*, 1996, **43**, 1739–1753.
56 L. D. Pettit and H. K. J. Powell, The IUPAC Stability Constants Database, Royal Society of Chemistry, London, 1992–2000.
57 L. Alderighi, P. Gans, A. Ienco, D. Peters, A. Sabatini, and A. Vacca, *Coord. Chem. Rev.*, 1999, **184**, 311–318.
58 R. A. Binstead, A. D. Zuberbühler, and B. Jung, 2004.
59 M. J. Frisch, G. W. Trucks, H. B. Schlegel, G. E. Scuseria, M. A. Robb, J. R. Cheeseman, J. Montgomery, T. Vreven, K. N. Kudin, J. C. Burant, J. M. Millam, S. S. Iyengar, J. Tomasi, V. Barone, B. Mennucci, M. Cossi, G. Scalmani, N. Rega, G. A. Petersson, H. Nakatsuji, M. Hada, M. Ehara, K. Toyota, R. Fukuda, J. Hasegawa, M. Ishida, T. Nakajima, Y. Honda, O. Kitao, H. Nakai, M. Klene, X. Li, J. E. Knox, H. P. Hratchian, J. B. Cross, V. Bakken, C. Adamo, J. Jaramillo, R. Gomperts, R. E. Stratmann, O. Yazyev, A. J. Austin, R. Cammi, C. Pomelli, J. W. Ochterski, P. Y. Ayala, K. Morokuma, G. A. Voth, P. Salvador, J. J. Dannenberg, V. G. Zakrzewski, S. Dapprich, A. D. Daniels, M. C. Strain, O. Farkas, D. K. Malick, A. D. Rabuck, K. Raghavachari, J. B. Foresman, J. V Ortiz, Q. Cui, A. G. Baboul, S. Clifford, J. Cioslowski, B. B. Stefanov, G. Liu, A. Liashenko, P. Piskorz, I. Komaromi, R. L. Martin, D. J. Fox, T. Keith, M. A. Al-Laham, C. Y. Peng, A. Nanayakkara, M. Challacombe, P. M. W. Gill, B. Johnson, W. Chen, M. W. Wong, C. Gonzalez, and J. A. Pople, Gaussian, Inc., Wallingford CT, 1993.
60 A. D. Becke, *J. Chem. Phys.*, 1993, **98**, 5648–5652.
61 A. D. Becke, *Phys. Rev. A At. Mol. Opt. Phys.*, 1988, **38**, 3098–3100.
62 K. D. Dobbs and W. J. Hehre, *J. Comput. Chem.*, 1987, **8**, 861–879.

View Article Online
DOI: 10.1039/C4DT03264K

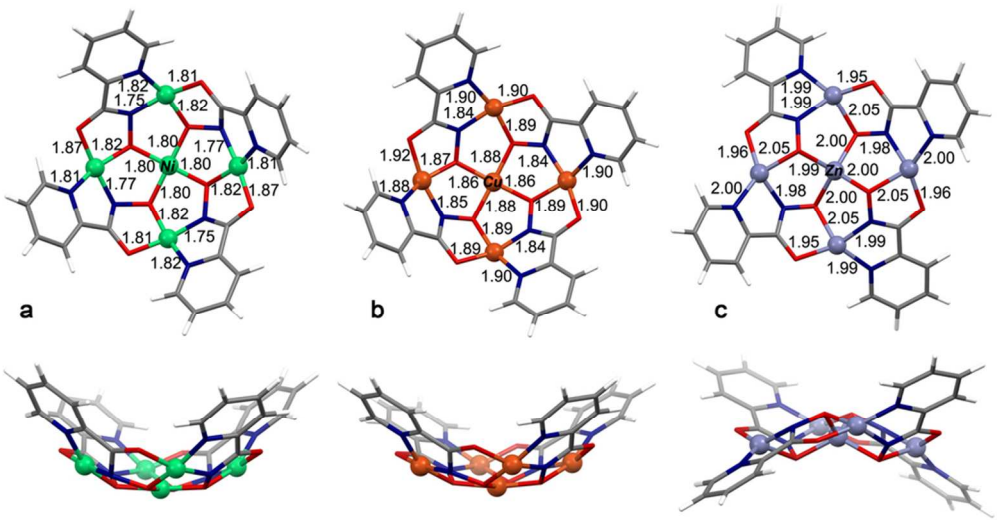

Figure 9. Depiction of the optimized molecular structures of the 12-MC-4 with Picha (HL) [Ni5(LH-1)4]2+ (a), [Cu5(LH-1)4]2+ (b), and [Zn5(LH-1)4]2+ (c) with relevant bond distances (Å). Top view (above) and side view (below). B3LYP/3-21G.

88x45mm (300 x 300 DPI)